electronics

MDPI

Article

Parametric Analysis of Linear Periodic Arrays Generating Flat-Top Beams

Piero Angeletti [1], Giulia Buttazzoni [2], Giovanni Toso [1,*] and Roberto Vescovo [2]

[1] RF Payloads and Technology Division, European Space Agency, 2200 Noordwijk, The Netherlands; piero.angeletti@esa.int
[2] Department of Engineering and Architecture, University of Trieste, Via A. Valerio 10, 34127 Trieste, Italy; gbuttazzoni@units.it (G.B.); vescovo@units.it (R.V.)
* Correspondence: giovanni.toso@esa.int

Abstract: Several synthesis techniques are available to optimize amplitude and phase excitations of periodic linear arrays to generate flat-top beams. Clearly, the optimal tapering depends on design parameters such as the array length, the number of array elements, the beam flatness, the beam width, the side lobe levels, and others. In this paper, in order to derive useful guidelines and rule of thumb for the synthesis of periodic array antennas, relations between these parameters are derived employing linear programming techniques, which guarantee optimality of the solutions. Such relations are then plotted and used in some design examples.

Keywords: array antennas; array synthesis; linear programming; periodic arrays

Citation: Angeletti, P.; Buttazzoni, G.; Toso, G.; Vescovo, R. Parametric Analysis of Linear Periodic Arrays Generating Flat-Top Beams. *Electronics* **2021**, *10*, 2452. https://doi.org/10.3390/electronics10202452

Academic Editors: Iván González and Lorena Lozano Plata

Received: 1 July 2021
Accepted: 5 October 2021
Published: 9 October 2021

1. Introduction

In this paper, the canonical problem of generating a flat-top beam with a linear array of equally spaced identical elements is investigated. A flat-top beam is a radiation pattern having an intensity profile that is flat over a required region of interest. Several antenna applications, such as reconnaissance and search RADARs, and wide-area broadcasting communication systems, require flat-top beams characterized by well-defined beamwidths. For such applications, key radiation pattern requirements are the ripple within the main-beam and the level of sidelobes after a transition zone from the main beam. Well-established synthesis procedures such as Fourier [1] or Woodward–Lawson [2,3] exist but are not particularly well suited due to the Gibbs phenomenon. Inspired by Butterworth filters [4], Ksienski introduced an analytical procedure [5] (extended in [6]) which maximizes the smoothness of the radiation patter at the expenses of an enlarged transition zone. Notwithstanding their speed, these techniques result suboptimal due to the unnecessary constraint on the realness of the voltage radiation pattern. In this respect, linear programming techniques allow for finding the global optimal solution to the flat-top power pattern problem [7].

Given an array geometry (i.e., the elements positions), the problem of the optimization of array excitations to satisfy arbitrary upper and lower bounds for the main beam and sidelobes is casted in the equivalent problem of the optimization of the real and imaginary parts of the autocorrelation of the excitations, which become the new unknowns. In this auxiliary space, the power pattern is a linear transformation of the unknowns (as the voltage pattern is a linear function of the array excitations) and the power pattern constraints can be described as linear constraints on the unknowns (an additional linear constraint on the positivity of the power pattern must be added). The goodness of this transposition stays in the fact that the minimization of the sidelobes and/or of the main-beam ripple become convex problems admitting a unique global solution, which can be found with linear programming techniques. Although the formulation [7] used in the following sections leverages on the framework developed by L. R. Rabiner in 1972 for

Finite-Impulse-Response (FIR) filters [8,9], the application to array antennas and optimality aspects can be found in [10].

Concerning the computational speed of linear programming solvers, while the theoretical analyses of their complexity remain an open problem, the simplex method or the interior point methods have been shown to exhibit typical polynomial (in the number of unknowns and constraints) running times (which correspond to few seconds in the instances of the addressed problem) [11]. Notwithstanding the global optimality of the linear programming solution for a specified flat-top-beam problem, the sensitivity of the solution to the input parameters has not been addressed in the technical literature (to the best knowledge of the authors). This paper analyzes the performance relationships between the following design parameters: array length, number of array elements, beam width, maximum allowed beam ripple, and width of the transition region between the main beam and the side lobes. Adopting a linear programming approach, the optimal value of the maximum side lobe level is derived and graphically illustrated as a function of the other parameters. The study presented in this paper does not aim to propose a new array synthesis algorithm but rather to deepen the analyses presented in [7] to provide antenna engineers with some design curves giving useful insights in the problem and data for the preliminary phase of synthesis.

In addition to the analytical methods [1–6], the literature offers a great variety of numerical methods for the array synthesis. As an example, in [12–14], deterministic procedures are proposed based on alternating projection approaches; in [15], a linear programming optimization plus a polynomial factorization is conceived; and [16] proposes a fast and versatile deterministic algorithm that iteratively minimizes a suitable weighted cost function. Furthermore, many global optimization techniques have been proposed, such as those presented in [17,18], based on genetic algorithms; the one proposed in [19], based on the differential evolution algorithm; and that in [20], which exploits the particle swarm optimization approach. Although this canonical problem has been already investigated, to the knowledge of the authors, attention has never been focused on the relations between the abovementioned design parameters. The authors believe that such an analysis may be very useful in the preliminary phase of design. For example, using the curves shown in Section 3, the antenna designer can estimate the length of the linear array necessary to achieve certain assigned performances or can anticipate the expected pattern characteristics of a flat-top beam realizable with an array having a given length.

The paper is organized as follows. In Section 2 the problem is formulated. In Section 3 the dependence of the maximum side lobe level on various design parameters is presented and discussed along with an asymptotical analysis aimed to verify the results with respect to the number of pattern samples utilized to derive the relations between the design parameters. In Section 4 some numerical examples are presented in order to describe how the reference curves can be used and to prove the superiority of the linear programming compared with conventional methods for the synthesis of shaped beams. The conclusions are proposed in Section 5.

2. Formulation of the Problem

The array factor of a linear antenna array of N identical equally spaced elements is given by the following:

$$F(\vartheta) = \sum_{n=0}^{N-1} E_n e^{jk_0 ndu} \quad (1)$$

where E_n is the excitation of the n-th element; $j = \sqrt{-1}$; $k_0 = 2\pi/\lambda$, with λ the wavelength; d is the inter-element spacing; and $u = \sin\theta$, where θ is the angle from broadside. In the sequel, the power pattern $|F(\vartheta)|^2$ will be considered.

A flat-top beam pattern can be characterized by the main beam edge u_{MB}, the ripple δ_{MB} in the main beam, the maximum side lobe level δ_{SL}, and the side lobe edge u_{SL}, as depicted in Figure 1. The additional parameters $\Delta u = u_{SL} - u_{MB}$ and $K = \delta_{MB}/\delta_{SL}$ are also introduced.

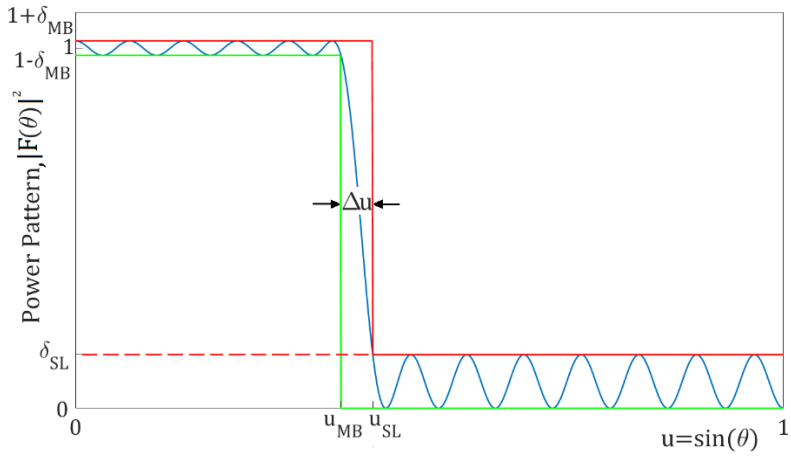

Figure 1. Example of a constraints compliant radiation pattern and definition of the design parameters u_{MB}, u_{SL}, δ_{MB}, δ_{SL}, and Δu for the flat-top power pattern.

The aim of the investigation presented in this paper is to derivie the relations between the above design parameters, exploiting them in the synthesis of flat-top beams. With this in mind, the desired values of u_{MB}, u_{SL} (or, alternatively, Δu), and δ_{MB} (or, alternatively, K) are imposed, and the power pattern is calculated in such a way as to satisfy the constraints imposed on these parameters, simultaneously minimizing the maximum side lobe level δ_{SL}. This problem is solved by using a linear programming approach, as briefly explained below (see [8,9] for further details). At first, the power pattern is written as follows:

$$|F(\vartheta)|^2 = \sum_{n=-(N-1)}^{N-1} R_n e^{jk_0 ndu} \tag{2}$$

where

$$R_n = \begin{cases} \sum_{i=n}^{N-1} E_i E_{i-n}^* \;\; if \; 0 \le n \le (N-1) \\ \sum_{i=-n}^{N-1} E_i^* E_{i+n} \; if \; -(N-1) \le n < 0 \end{cases} \tag{3}$$

with the asterisk denoting complex conjugate. By (3), $R_{-n} = R_n^*$. Therefore, (2) can be written in the following form:

$$|F(\vartheta)|^2 = A_0 + 2\sum_{n=1}^{N-1}(A_n \cos(k_0 ndu) - B_n \sin(k_0 ndu)), \tag{4}$$

with $R_n = A_n + jB_n$ and in particular $R_0 = \sum_{i=0}^{N-1}|E_i|^2 = A_0$. The design parameters u_{MB}, u_{SL}, δ_{MB}, and δ_{SL} are then used to define a mask for the power pattern in (2). Such a mask is illustrated in Figure 1. Thanks to the auxiliary variables R_n in (2) and (3), the power pattern synthesis is formulated as a linear programming problem, where the objective function to be minimized is δ_{SL}. The problem can be formulated as follows:

$$\text{minimize}\{\delta_{SL}\}$$

subject to the following constraints:

$$-|F(u)|^2 \le -L(u) \tag{5a}$$

$$|F(u)|^2 \le U(u) \tag{5b}$$

$$-\delta_{SL} \le 0 \tag{5c}$$

$$\delta_{MB} = \delta_{MB}^{des} \; or \; \delta_{SL} = \delta_{MB}/K^{des} \tag{5d}$$

where $L(u)$ and $U(u)$ are two positive functions representing, respectively, the lower and the upper bound of the mask, and are defined as

$$L(u) = (1 - \delta_{MB})LE(u, u_{MB}) \tag{6a}$$

$$U(u) = (1 + \delta_{MB} - \delta_{SL})LT(u, u_{SL}) + \delta_{SL} \tag{6b}$$

Note that the constraints in (5) impose that the power pattern belong to the mask specified by $L(u)$ and $U(u)$ (conditions (5a) and (5b)), in which $\delta_{SL} \geq 0$ (condition (5c)), and impose a desired value to δ_{MB} or, alternatively, to K (condition (5d)). The solution of the linear programming problem in (5) provides the values of the variables R_n of an equi-ripple power pattern, which perfectly fits between the lower and upper masks and exhibits the minimum attainable δ_{SL}.

In the next section, several curves representing the relations between the design parameters are illustrated. Such results are obtained by sampling the synthesized radiation patterns on a set of equally spaced points in the visibility interval $[-1; 1]$. Subsequently, the asymptotic behavior of the results is numerically analyzed by adopting an increasing number of samples. Three examples of array synthesis are presented in Section 4, and are solved with the aid of the obtained curves involving the design parameters.

3. Maximum Sidelobe Level vs. Design Parameters

In the sequel, a linear array with inter-element spacing $d = \lambda/2$ will be considered, and the dependence of the maximum side lobe level on the other design parameters is derived and plotted for some test cases, by using the above described linear programming approach.

3.1. Case of Equality between Main Beam Width and Side Lobe Region Width

First, let us analyze the case where the main beam width (u_{MB}) is equal to the side lobe region width ($1 - u_{SL}$), that is $u_{MB} + u_{SL} = 1$, and in (5d) $K^{des} = \delta_{MB}/\delta_{SL} = 1$ (i.e., $\delta_{MB} = \delta_{SL} = \delta$). Figure 2 shows δ as a function of the transition width Δu. In the figure, different curves refer to different values of N. As expected, higher values of Δu correspond to lower values of δ as well as higher values of N correspond to lower values of δ. Thus, lower side lobes can be obtained with larger arrays or by allowing for a larger transition region.

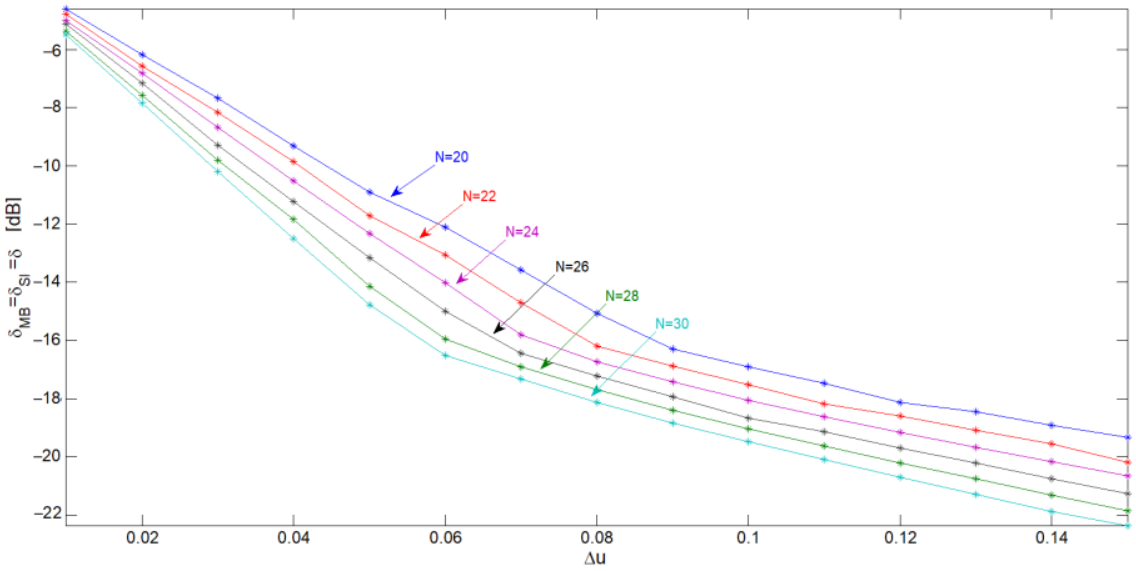

Figure 2. Case of equality between the main beam width and the side lobe region width, and $K^{des} = \delta_{MB}/\delta_{SL} = 1$: the curves show $\delta = (\delta_{MB} = \delta_{SL})$ as a function of Δu for N taking values from 20 to 30.

From now on, unlike the previous case, flat-top beams are considered with u_{MB} and $1 - u_{SL}$ possibly different, and δ_{MB} possibly different from δ_{SL} (i.e., $K^{des} \neq 1$).

3.2. Dependence on N

Figure 3a,b show the maximum side lobe level δ_{SL} as a function of N. Both figures refer to the case $u_{MB} = 0.375$. As expected, the more stringent the constraints (that is, the values of Δu and δ_{MB} are lower), the higher the obtained values of maximum side lobe levels. The curves in Figure 3a are obtained with $\delta_{MB} = 0.1$ and Δu = 0.05, 0.1, 0.15, whereas those in Figure 3b refer to the case $\Delta u = 0.1$ and $\delta_{MB} = 0.02,\ 0.1,\ 0.2$. In both figures, the curves show a quasi-linear behavior. However, the curves in Figure 3b exhibit nearly the same slope, unlike those in Figure 3a.

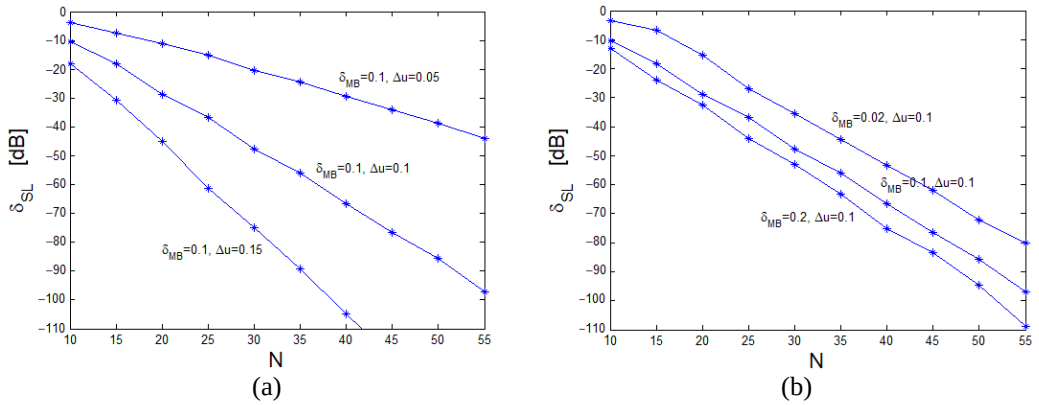

Figure 3. Maximum side lobe level δ_{SL} (in dB) as a function of N, obtained with $u_{MB} = 0.375$ and: (**a**) a common value of $\delta_{MB} = 0.1$ and varying Δu; (**b**) a common value of $\Delta u = 0.1$ and varying δ_{MB}.

3.3. Dependence on K

The dependence of the maximum side lobe level δ_{SL} on $K(= \delta_{MB}/\delta_{SL})$ is analyzed here. In the next three figures, the same main beam edge $u_{MB} = 0.5$ is considered, and the maximum side lobe level decreases as K increases. In Figure 4a, which corresponds to $\Delta u = 0.2$, all curves are practically linear. Instead, in Figure 4b, corresponding to $\Delta u = 0.15$, for high values of K, the curve obtained for $N = 20$ is nonlinear. In Figure 4c, corresponding to $\Delta u = 0.1$, the behavior is quasi-linear only for $N = 40$.

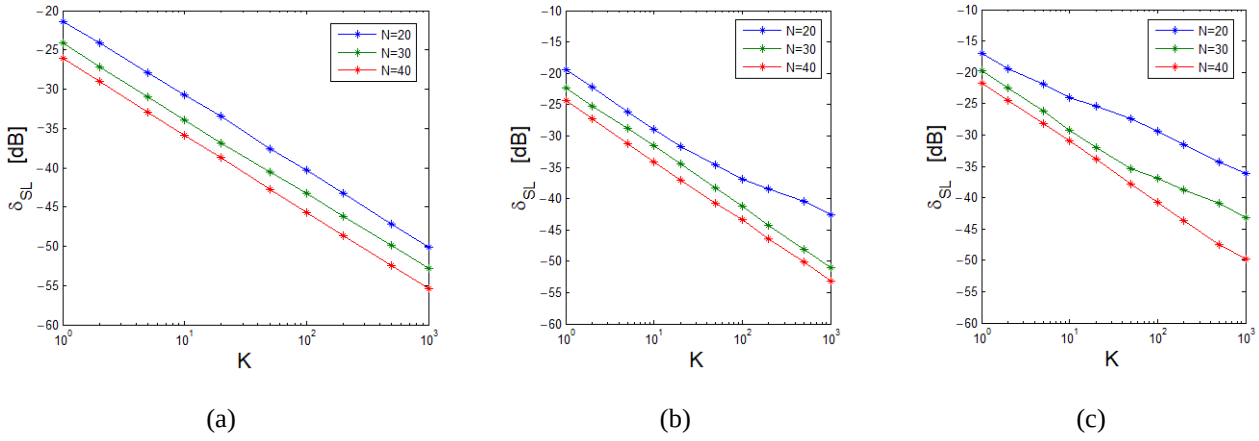

Figure 4. Maximum side lobe level δ_{SL} (in dB) as a function of K. The curves are obtained for $u_{MB} = 0.5$ and (**a**) $\Delta u = 0.2$, (**b**) $\Delta u = 0.15$, and (**c**) $\Delta u = 0.1$.

3.4. Dependence on δ_{MB}

Figure 5 shows the maximum side lobe level as a function of δ_{MB}, through the parameter $\tau_{MB} = (1 + \delta_{MB})/(1 - \delta_{MB})$ expressed in dB (the parameter τ_{MB} is used in agreement with several other papers, for example [9]). As expected, the maximum side lobe level is lower for higher values of δ_{MB}: in other words, when relaxing the requirements for the maximum allowed ripple amplitude in the main beam, a reduction in the maximum side lobe level is observed. Moreover, the different curves refer to different values of Δu. All curves have nearly the same shape and show that larger transition regions permit achieving better side lobe levels. All curves refer to the case $u_{MB} = 0.46$ and $N = 20$.

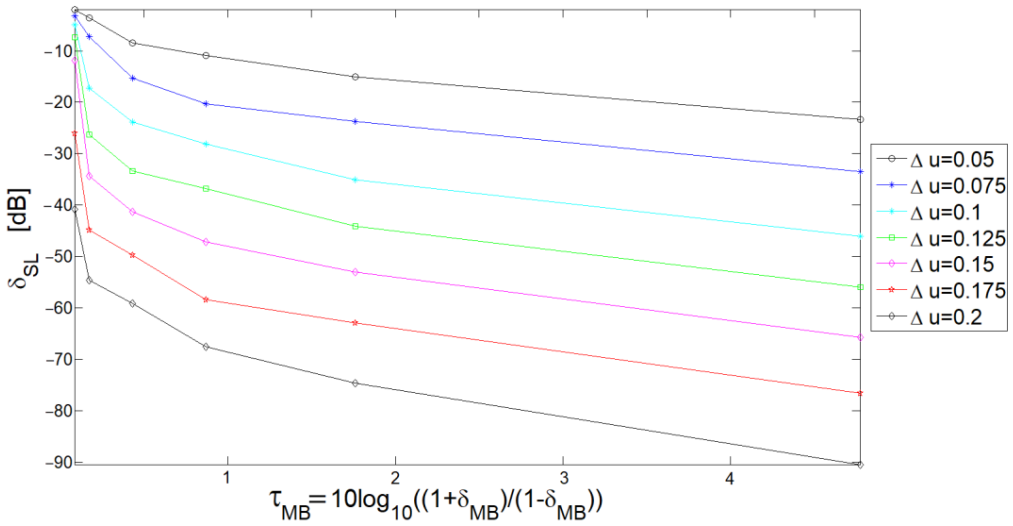

Figure 5. Case Maximum side lobe level δ_{SL} (in dB) as a function of the parameter $\tau_{MB} = (1 + \delta_{MB})/(1 - \delta_{MB})$ expressed in dB, where δ_{MB} is the maximum allowed ripple amplitude, in the case where $N = 20$ and $u_{MB} = 0.46$, with different values of Δu ranging from 0.05 to 0.2.

3.5. Dependence on u_{MB}

Figure 6a shows the maximum side lobe level δ_{SL} as a function of u_{MB} for a maximum allowed beam ripple $\delta_{MB} = 0.05$ and a transition region Δu varying from 0.05 to 0.2. As expected, larger transition regions globally allow for lower maximum side lobe levels, but δ_{SL} does not vary monotonically as a function of u_{MB}: all curves show the same behavior, with alternating maxima and minima. However, the average slope of the curves and the differences between maxima and minima tend to increase when increasing of Δu.

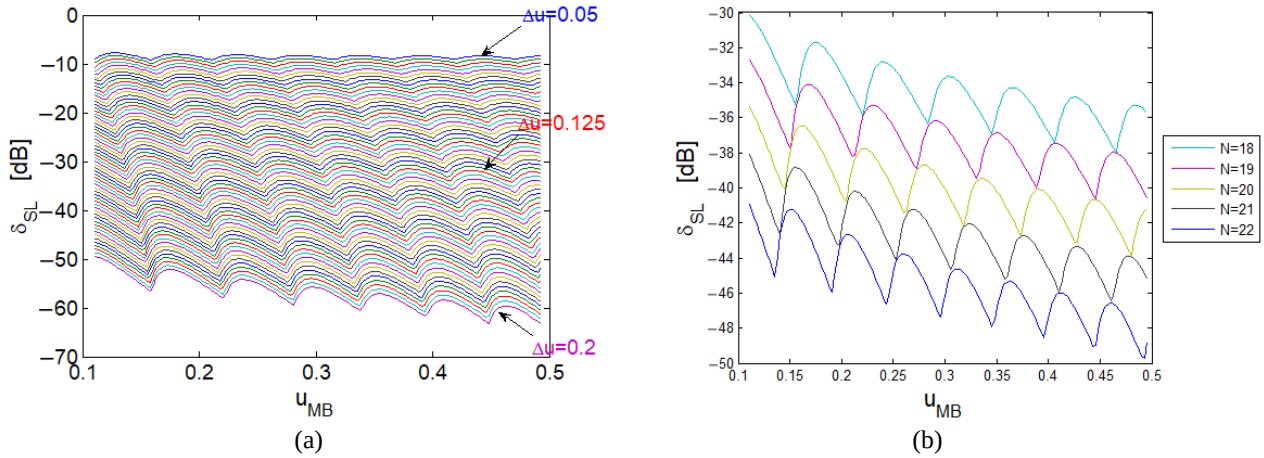

Figure 6. Maximum side lobe level δ_{SL} (in dB) as a function of u_{MB}, obtained for $\delta_{MB} = 0.05$ and (**a**) $N = 20$ with Δu =0.05, 0.125, 0.2, (**b**) $\Delta u = 0.15$ with N from 18 to 22.

Figure 6b shows the maximum side lobe level as a function of the main beam edge u_{MB} for an assigned beam ripple $\delta_{MB} = 0.05$. All of the curves in the figure refer to a transition region $\Delta u = 0.15$ and to different values of N, varying from $N = 18$ to $N = 22$. It is interesting to note that all curves show a similar behavior. As expected, lower side lobe levels can be obtained with higher values of N. However, for certain values of u_{MB}, corresponding to the minima along the curve obtained with N elements, the corresponding values of δ_{SL} are nearly coincident with the values obtained with $N + 1$ elements. Moreover, for low values of u_{MB}, the maximum of the curve corresponding to N elements is higher compared with the closest minimum of the curve with $N + 1$ elements.

3.6. Dependence on δ_{MB}

Figure 7 shows the maximum side lobe level as a function of the transition region Δu for $u_{MB} = 0.16$ and different values of δ_{MB} from 0.01 to 0.5. All curves are decreasing, but their behavior is not linear. Observe that the light blue curve, corresponding to $\delta_{MB} = 0.05$, contains the same values obtainable when sampling the curves in Figure 6a for $u_{MB} = 0.16$.

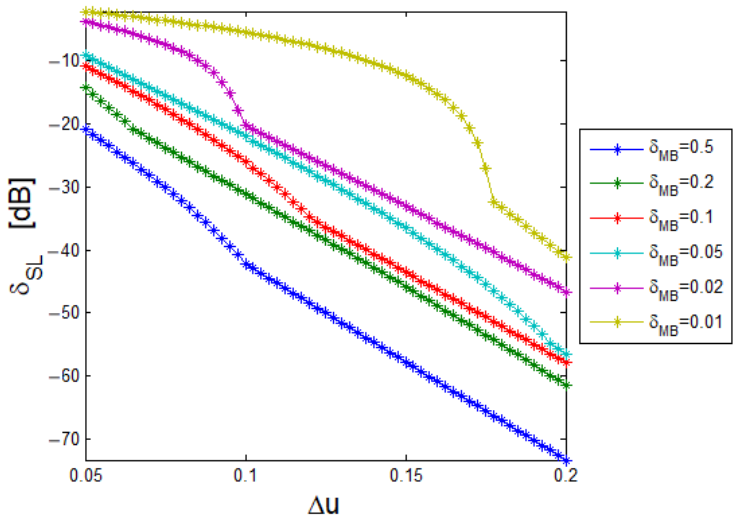

Figure 7. Maximum side lobe level δ_{SL} (in dB) as a function of Δu, for $N = 20$, $u_{MB} = 0.16$ and δ_{MB} varying from 0.5 to 0.01.

3.7. Asymptotical Analysis

The above numerical results have been obtained by sampling the power patterns on a grid of $N_s = 800$ equally spaced points in the interval $[-1; 1]$. In order to verify the asymptotic stability of the results, we applied the adopted method of synthesis and re-calculated the above curves using different numbers N_s of samples. For example, with reference to the already discussed Figure 7, which corresponds to $N = 20$ and $u_{MB} = 0.16$, we set $\delta_{MB} = 0.1$ and analyzed the dependence of δ_{SL} on Δu for N_s going from 200 to 3200. Figure 8 shows the results obtained.

Different curves correspond to different values of N_s. As it can be seen, the results nearly independent of the number of samples. In order to better illustrate the convergence, Figure 9 shows the maximum side lobe level as a function of the number of samples for $N = 20$, $u_{MB} = 0.16$, and $\Delta u = 0.7$. Note that the curve tends to saturate rapidly when increasing the number of samples. Thus, the results prove the effectiveness of the adopted method to calculate the relations between the design parameters, showing a behavior quasi-independent of the number of points on which the power patterns have been sampled.

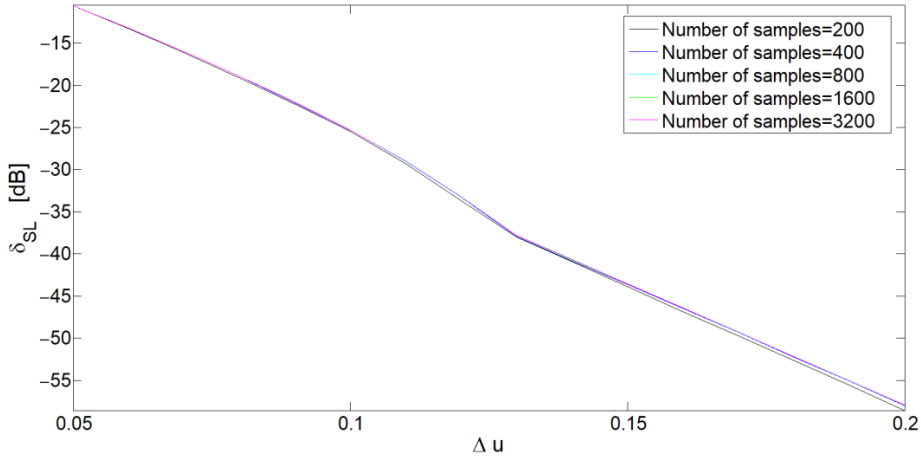

Figure 8. Maximum side lobe level δ_{SL} (in dB) as a function of Δu, for $N = 20$, $u_{MB} = 0.16$, and the number of sampling points varying from 200 to 3200.

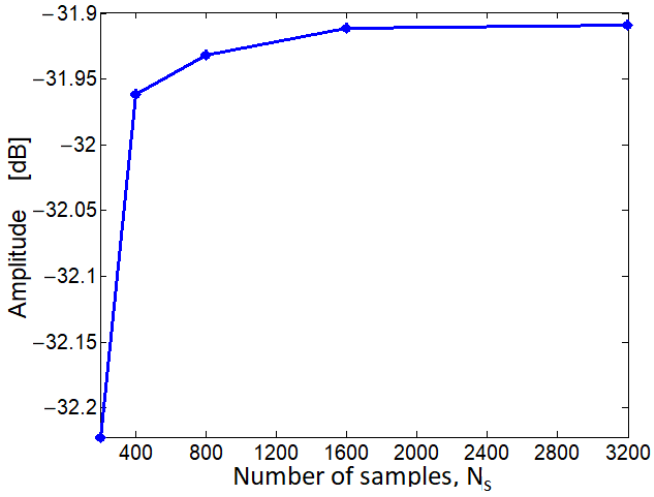

Figure 9. Maximum side lobe level (in dB) as a function of the number of samples, for $N = 20$, $u_{MB} = 0.16$, and $\Delta u = 0.7$.

4. Examples

In this section, three significant examples are proposed, which show how the above derived curves can help in the preliminary design phase of linear antenna arrays radiating flat-top beams.

4.1. First Example: Case of Equality between Main Beam Width and Side Lobe Region Width

Let us assume that a linear array composed by $N = 30$ elements is required to radiate a flat-top beam, with the main beam region and the side lobe region having the same width (i.e., $u_{MB} + u_{SL} = 1$), and $K = 1$ (i.e, $\delta_{MB} = \delta_{SL} = \delta$). We want to find the maximum beam width (or, equivalently, the minimum transition region Δu), which guarantees a maximum side lobe level $\delta_{SL} \leq -15$ dB. Using the curve corresponding to $N = 30$ in Figure 2, we can observe that a value $\Delta u = 0.055$ can give a power pattern satisfying the required specifications. In fact, using the linear programming with $u_{MB} = 0.5 - \frac{\Delta u}{2} = 0.4725$, $u_{SL} = 0.5 + \frac{\Delta u}{2} = 0.5275$, and $K = 1$, we obtain the radiation pattern of Figure 10a, with a maximum side lobe level of -15.68 dB and a maximum allowed ripple in the main beam (shown in the inset of Figure 10a) of $\delta = 0.027$, which corresponds to $\tau_{MB} = 10 \log_{10}((1+\delta)/(1-\delta)) = 0.23$. The CPU time for this example is approximately 0.1 s.

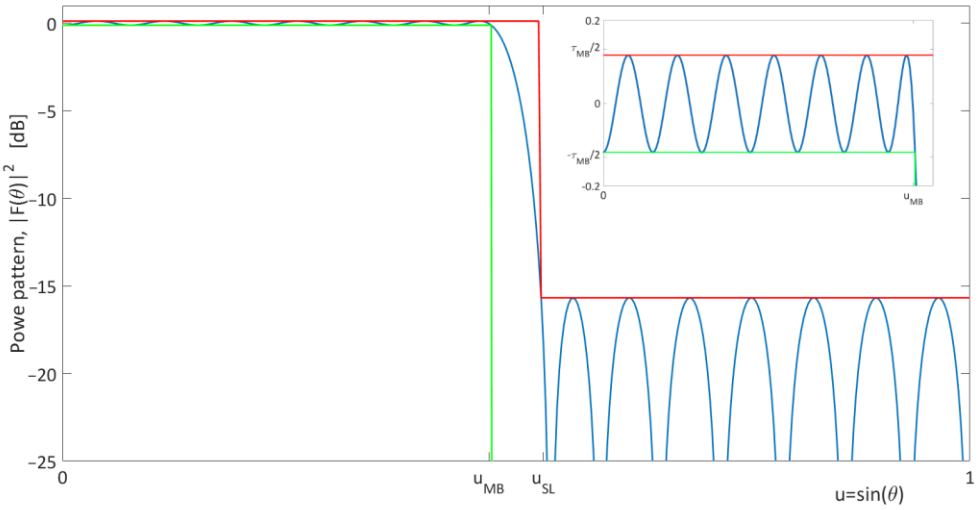

(a)

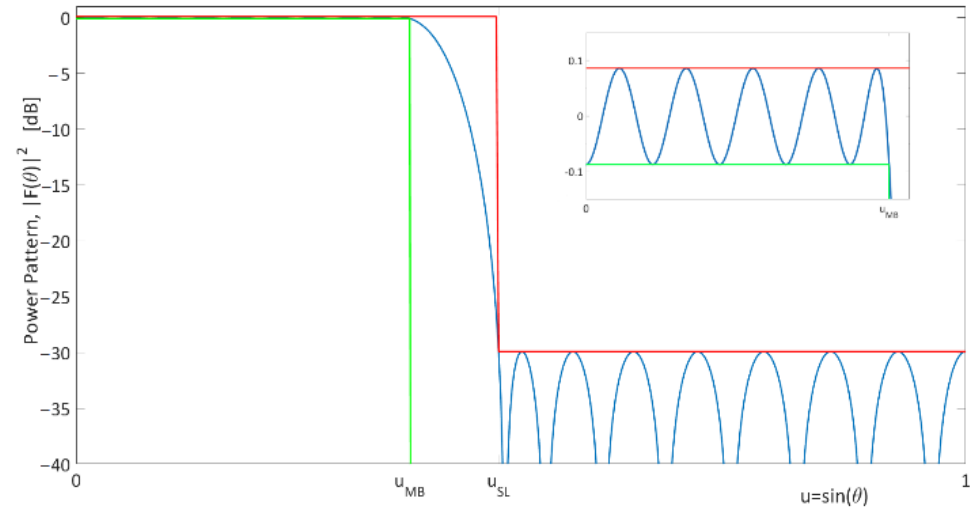

(b)

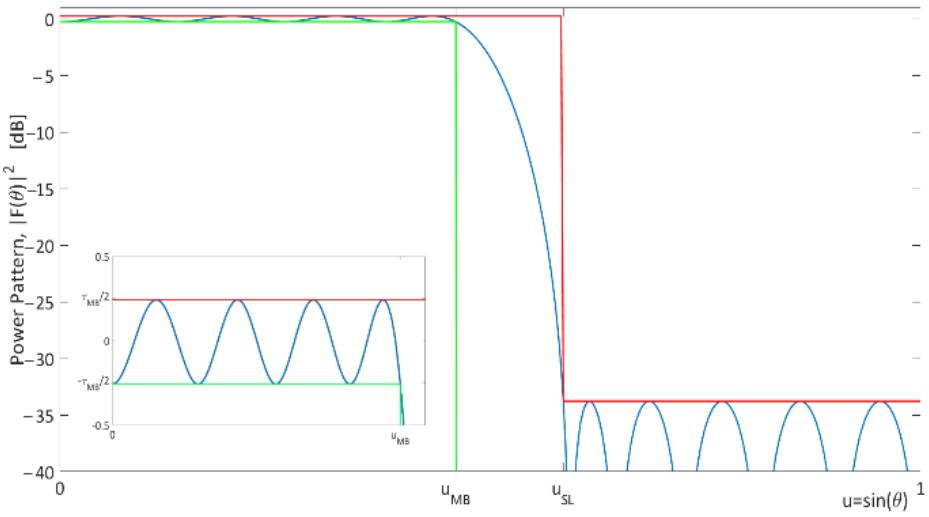

(c)

Figure 10. The radiation patterns synthesized with the linear programming for the examples in (**a**) Section 4.1, (**b**) Section 4.2, and (**c**) Section 4.3. All of the patterns satisfy the imposed constraints.

4.2. Second Example: Estimation of the Number of Elements

As a second example, we want to produce a flat-top beam with the following values for the design parameters: $u_{MB} = 0.375$, $\Delta u = 0.1$, $\delta_{MB} = 0.02$, and $\delta_{SL} \leq -30$ dB. With the help of Figure 3b, we note that an array of $N = 27$ elements can achieve the required performances. In fact, using the linear programming with these parameters yields the power pattern of Figure 10b, which satisfies the constraints. The CPU time for this example is slightly lower than 0.1 s.

4.3. Third Example: Estimation of the Width of the Transition Region

Let us consider a linear antenna array composed by $N = 20$ elements. We want to radiate a flat-top beam with a beamwidth $u_{MB} = 0.46$, a maximum side lobe level of -30 dB and a maximum allowed ripple in the main beam region $\delta_{MB} = 0.0575$ ($\tau_{MB} = 0.5$ dB). The curves in Figure 5 suggest that a possible value of width of the transition region that allows us to satisfy the requirement is $\Delta u = 0.125$. In fact, using the linear programming with these parameters yields the power pattern in Figure 10c, which satisfies all of the constraints. The CPU time for this example is slightly lower than 0.1 s.

4.4. Result Comparison

This final subsection aims to prove the superiority of the adopted linear programming in terms of constraint compliance for the flat-top beam synthesis. Precisely, the previous three examples have been solved with two well-known methods, i.e., the Fourier Transform approach [1] and the Woodward–Lawson technique [2]. Figure 11 shows the patterns obtained by the three methods. As it can be seen, only the linear programming always satisfies the imposed constraints, whereas the classical methods may fail to meet the requirements. On the other hand, both the Woodward–Lawson technique and the Fourier Transform approach have the advantage of using closed-form expressions for the addressed problems. Thus, the CPU times are quite low (approximately 1 ms or even less).

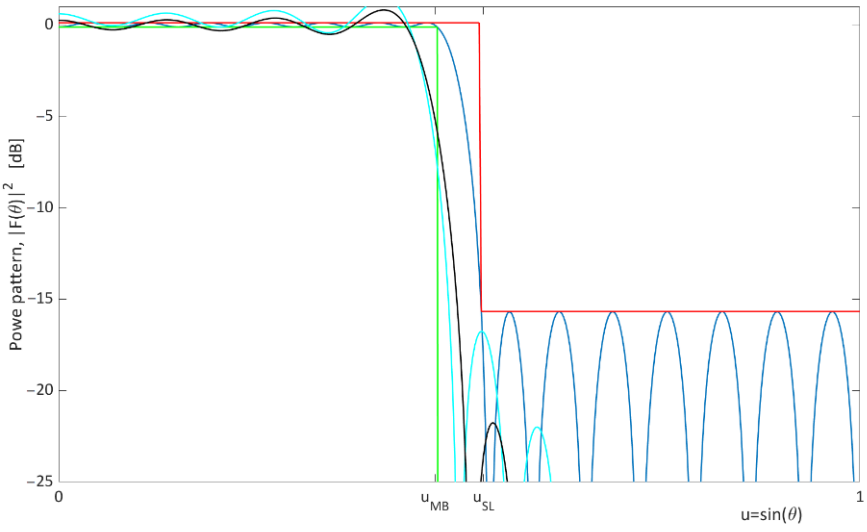

(a)

Figure 11. *Cont.*

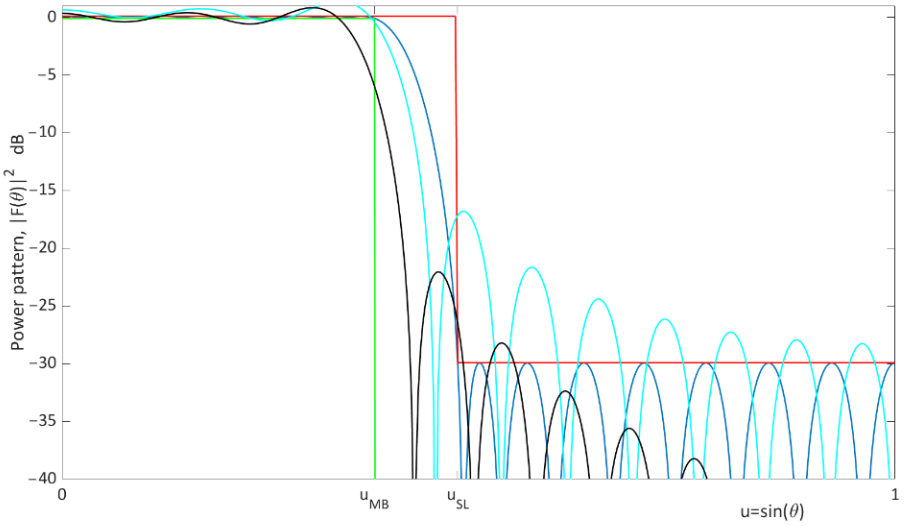

(b)

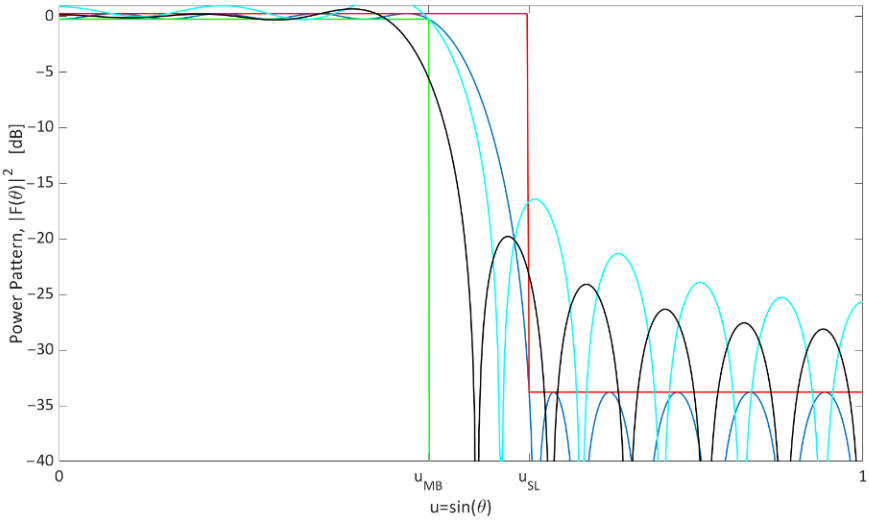

(c)

Figure 11. Comparison. The radiation patterns synthesized with the linear programming (blue lines), compared with the patterns of the Woodward–Lawson method (ciano lines) and those of the Fourier Transform approach (black lines) for the examples in (**a**) Section 4.1, (**b**) Section 4.2, and (**c**) Section 4.3. All of the patterns satisfy the imposed constraints.

5. Conclusions

The power synthesis of flat-top beams for linear periodic arrays is a well-known canonical problem in the antenna community. The shape of the synthesized pattern depends on a number of design parameters, such as the array length, the beam width, the maximum allowed ripple in the main beam region, the width of the transition region, and the maximum side lobe level.

The aim of this paper was to derive the relations between these design parameters and to use them for design purposes. Adopting a linear programming technique that guarantees the optimality of the solutions, several case studies were analyzed, obtaining a set of relations between the above parameters, which are represented graphically by curves that can be useful in the array design. Three examples of array design were proposed, and solved with the aid of these curves, obtaining results fully compliant with the assigned masks. In particular, the curves show that, also for the simple case of linear equally spaced

arrays, the relations between the design parameters can be nonlinear. This is an interesting and not completely expected result, which must be taken into account in the array design.

Author Contributions: P.A. and G.B.: conceptualization, review and editing, G.B.: conceptualization, software, and original draft preparation, G.T.: conceptualization, writing and validation, R.V.: conceptualization. All authors have read and agreed to the published version of the manuscript.

Funding: This research received no external funding.

Conflicts of Interest: The authors declare no conflict of interest.

References

1. Dunbar, A.S. On the Theory of Antenna Beam Shaping. *J. Appl. Phys.* **1952**, *23*, 847–853. [CrossRef]
2. Woodward, P.M. A Method for Calculating the Field Over a Plane Aperture Required to Produce a Given Polar Diagram. *J. Inst. Electr. Eng. Part IIIA Radiolocat.* **1946**, *93*, 1554–1558. [CrossRef]
3. Woodward, P.M.; Lawson, J.D. The theoretical precision with which an arbitrary radiation pattern may be obtained from a source of a finite size. *J. Inst. Electr. Eng. Part III Radio Commun. Eng.* **1948**, *95*, 363–370.
4. Butterworth, S. On the theory of filter amplifiers. *Exp. Wirel.* **1930**, *7*, 536–541.
5. Ksienski, A. Maximally flat and quasi-smooth sector beams. *IRE Trans. Antennas Propag.* **1960**, *8*, 476–484. [CrossRef]
6. Petrolati, D.; Angeletti, P.; Toso, G. Linear arrays with Maximally Flat Beams. In Proceedings of the Fourth European Conference on Antennas and Propagation, Barcelona, Spain, 12–16 April 2010.
7. Angeletti, P.; Buttazzoni, G.; Toso, G.; Vescovo, R. Parametric analysis of flat top beam patterns generated by linear periodic arrays. In Proceedings of the 2016 10th European Conference on Antennas and Propagation (EuCAP), Davos, Switzerland, 10–15 April 2016; pp. 1–2.
8. Rabiner, L.R. Linear program design of finite impulse response (FIR) digital filters. *IEEE Trans. Audio Electroacoust.* **1972**, *20*, 280–288. [CrossRef]
9. Rabiner, L.R. The design of finite impulse response digital filters using linear programming techniques. *Bell Syst. Tech. J.* **1972**, *51*, 1177–1198. [CrossRef]
10. Isernia, T.; Bucci, O.M.; Fiorentino, N. Shaped beam antenna synthesis problems: Feasibility criteria and new strategies. *J. Electromagn. Waves Appl.* **1998**, *12*, 103–138. [CrossRef]
11. Karmarkar, N. A new polynomial-time algorithm for linear programming. *Combinatorica* **1984**, *4*, 373–395. [CrossRef]
12. Bucci, O.M.; D'Elia, G.; Mazzarella, G.; Panariello, G. Antenna pattern synthesis: A new general approach. *Proc. IEEE* **1994**, *82*, 358–371. [CrossRef]
13. Quijano, J.L.A.; Vecchi, G. Alternating adaptive projections in antenna synthesis. *IEEE Trans. Antennas Propag.* **2010**, *58*, 727–737. [CrossRef]
14. Buttazzoni, G.; Vescovo, R. An efficient and versatile technique for the synthesis of 3D copolar and crosspolar patterns of phase-only reconfigurable conformal arrays with DRR and near-field control. *IEEE Trans. Antennas Propag.* **2014**, *62*, 1640–1651. [CrossRef]
15. Isernia, T.; Morabito, A.F. Mask-constrained power synthesis of linear arrays with even excitations. *IEEE Trans. Antennas Propag.* **2016**, *64*, 3212–3217. [CrossRef]
16. Comisso, M.; Buttazzoni, G.; Vescovo, R. Reconfigurable antenna arrays with multiple requirements: A versatile 3D approach. *Int. J. Antennas Propag.* **2017**, *2017*, 6752108. [CrossRef]
17. Johnson, J.M.; Rahmat-Samii, Y. Genetic algorithms in engineering electromagnetics. *IEEE Antennas Propag. Mag.* **1997**, *39*, 7–21. [CrossRef]
18. Haupt, R.L. Antenna design with a mixed integer genetic algorithm. *IEEE Trans. Antennas Propag.* **2007**, *55*, 577–582. [CrossRef]
19. Yang, S.; Gan, Y.B.; Khiang, T.P. A new technique for power-pattern synthesis in time-modulated linear arrays. *IEEE Antennas Wirel. Propag. Lett.* **2003**, *2*, 285–287. [CrossRef]
20. Zhou, R.; Sun, J.; Wei, S.; Wang, J. Synthesis of conformal array antenna for hypersonic platform SAR using modified particle swarm optimization. *IET Radar Sonar Navig.* **2017**, *11*, 1235–1242. [CrossRef]